Toughening of Graphite–Epoxy Composites with an Electrocopolymerized High-Temperature Thermoplastic Interphase

ANGEL S. WIMOLKIATISAK* and JAMES P. BELL

Polymer Science Program, Institute of Materials Science, University of Connecticut, Storrs, Connecticut 06269-3136

SYNOPSIS

Electrocopolymerization of a high-temperature 3-carboxyphenylmaleimide-styrene interphase onto graphite fibers was carried out in an effort to toughen graphite–epoxy composites. The effects of the interphase and its thickness on the mechanical properties and the failure modes were investigated. The optimum interphase thickness was found to be about 0.16 μm. At this thickness, the average value of the DCB Mode I critical strain energy release rate is improved by about 100%, the average notched Izod impact resistance is improved by about 60%, and the average interlaminar shear strength is maintained at about the same value as the control composites. The failure mode was shifted toward more ductile failure with the inclusion of an interphase. © 1992 John Wiley & Sons, Inc.

INTRODUCTION

Toughening of many graphite–epoxy composites is highly desirable due to their relatively brittle nature. However, attempts to toughen these composites have usually resulted in a tradeoff between the toughness and the shear strength.[1-6] This has prompted many researchers to work on optimizing the interfacial adhesion,[7] resulting in a compromise between the two properties. Others have approached the problem by rubber-toughening the brittle matrix while holding a strong fiber-matrix adhesion,[8-18] or by hybridizing ductile fibers with brittle fibers.[19-22] Recently, increasing interest has been paid to other approaches such as (a) switching from brittle thermosetting matrices to high-performance, tougher thermoplastic matrices,[23-29] (b) the use of interpenetrating network matrices that offer improved toughness and easy processing,[30-45] and (c) the application of a tough interfacial interlayer or interphase onto the fibers before the matrix impregnation.[1-5,46-61] In general, these approaches have been more or less successful in imparting toughness and/or shear strength to the materials. Research on all these approaches is still ongoing.

For a number of years now, a research effort has been established in our laboratory to investigate the use of an electrocopolymerized interphase to toughen brittle graphite–epoxy composites, while maintaining or improving the interfacial or interlaminar shear strength. The idea in this approach is to use the tough polymer coatings (which can form strong physical and/or chemical bonds with the matrix) to absorb the impact energy. The advantages of such coatings on the composite properties are: (a) the interphase can absorb the crack propagation energy and blunt the crack tip, (b) the interphase is capable of relieving the stress concentration around the fibers, which results from the curing process or from the external applied load, and (c) the interphase can heal the fiber surface flaws and help to protect the brittle fibers from breaking when being handled. Details of these advantages have been discussed.[1,2,53-56] This interphase approach has been demonstrated to be effective for low glass transition temperature (T_g) acrylic interphases.[2,56,58]

* To whom correspondence should be addressed. Present address: Polymer Technology Group, Corporate Research, Ferro Corporation, 7500 E. Pleasant Valley Road, Independence, OH 44131.

Journal of Applied Polymer Science, Vol. 46, 1899-1914 (1992)
 CCC 0021-8995/92/111899-16

Since advanced composites are often used in high-temperature applications, it is desirable for the interphase to withstand high temperature. It has been found that the composite toughness can be enhanced by the incorporation of high T_g thermoplastics in a thermosetting polymer in the form of a semi-interpenetrating network.[30-45] In the interphase toughening approach, a tough but high T_g interphase may provide for improved toughness, better temperature stability, better environmental resistance, and better stress transfer capacity. Ideally, the interphase should have perfect bonding at the interfaces, be able to absorb the impact and fracture energy efficiently, perform well at high temperatures and under hygrothermal conditions, and yet be easy to process. The recently electrocopolymerized 3-carboxyphenyl maleimide-co-styrene, 3cmi-s,[62] interphase should have many of the above features. Composites made from Hercules AS4 graphite fibers, using this copolymer as a matrix, have been found to have a T_g of about 227°C and are very tough.[62] The effects of 3cmi-s as an interphase on the mode I critical strain energy release rate (G_{IC}), the notched Izod impact resistance (IMPR), and the short-beam apparent interlaminar shear strength (ILSS) are reported in this work.

Electrocopolymerization

Electropolymerization or electroinitiated polymerization is a process in which the polymerization is achieved only when an electrical current is applied. Polymerization can occur either at the anode or the cathode. Polymerization can be initiated by anions, cations, free radicals, or other reactive intermediates. These ions or free radicals can be induced from the monomer itself or from other initiators that are present in the system, depending on the electrochemical nature of the system. Electroinitiated polymer can form on the surface of the electrode if the polymer is insoluble in the solvent system, or it can be dissolved in the electropolymerization solution.

Electropolymerization of various polymers and copolymers onto graphite fibers used for making advanced composites has received considerable attention in the last few years because of the following advantages over other coating techniques: (1) Polymerization occurs *in situ* on the fiber surface, which has the potential for chemical grafting of the polymer onto the surface for good interfacial adhesion. (2) Electropolymerization is a self-healing process. The polymerization rate is higher at areas where there is thinner or no polymer coating because these areas have higher current density. The benefit of this process is that the fiber surface can be evenly coated. (3) The reaction rate can be controlled very easily by simply adjusting the applied electrical current or potential. (4) The chemical and physical structure and properties of the polymer coatings can be controlled by using different monomers or comonomers and by applying different monomers at different time.

Electropolymerization has been achieved for many types of monomers, including vinyl monomers (notably acrylates and styrene),[46,47,63-66] phenols,[67-71] polyimide and its intermediates,[62,72,73] tetrahydrofuran,[74] caprolactam,[75] conductive pyrrole and other heterocyclic aromatic compounds,[76-80] and vinyl pyridine complexes of various metals such as iron.[81-84] Numerous review articles have been written on the electropolymerization process, indicating a broad interest in the subject.[85-98]

The conditions required for electropolymerization vary greatly, depending on the solubility of the monomers, the electrochemical potential of the monomers, the supporting electrolytes, the solvents, the applied potential or current, and the desired coating properties and thickness. The choice of monomers and their supporting electrolytes is usually based on the desired polymer properties and the solubility of the monomers and the polymer in the solution. Generally, it is desirable to conduct electropolymerization in a water medium because free-radical polymerization mechanism is likely to occur, which can yield high molecular weight coating onto the electrode. However, most organic monomers have very limited solubility in water. Therefore, experimentation to find a suitable solvent or co-solvent system may be needed.

Critical Strain Energy Release Rate, G_{IC}

Interlaminar delamination is one of the predominant types of damage in composite materials, particularly in composites with different ply orientations. In unidirectional composites, interlaminar delamination usually occurs because the interlaminar region (a region between two composite plies) has few or no reinforcing fibers. The absence of fibers often is caused by improper processing of the composites. However, weak interlaminar regions were observed even when the processing is optimized.[99-104]

Interlaminar delamination failure is observed in many types of tests including the impact resistance test and the short-beam shear test. Delamination failure is a strong function of the interlaminar fracture toughness and the transverse strength of the composites. Resistance to delamination can be characterized by the double-cantilever beam (DCB)

fracture energy test, which can be tested in mode I, mode II, or mode III. However, mode I is most often the weakest failure mode[105-111] and has received the most attention.[112-124] A mode I DCB test was used in this study.

R-Curve Effect

The G_{IC} at initiation has been proposed for use to characterize interlaminar fracture energy, in addition to the average G_{IC}, $\bar{G}_{IC}$.[125] It has been demonstrated that at higher crack length, fiber bridging from one ply to another usually occurs, resulting in higher apparent G_{IC} values as the crack length is increased. This increasing G_{IC} with increasing crack length is known as the R-curve effect. The initial G_{IC}, G_{ICinit}, can be determined by the compliance method.[124-126] The equation to do so is[124,127]

$$G_{IC} = (P^2/2b)(dC/da) \quad (1)$$

where P, a, b, and C are the load, crack length, sample width, and compliance, respectively. From linear beam theory, C is a linear function of a^3. Hence, a plot of C versus a^3 should yield a straight line with a slope equal to dC/da. However, sometimes a considerable amount of deviation from the straight line may occur, especially at the initial crack length region, as shown in Figure 1. Because of this deviation, only the first several data points at the low crack length region were used in this study for the straight line fitting used in determining G_{ICinit}. The average G_{IC} was determined by an area method[123] using all the data except the first several data in the short crack length region. Both $\bar{G}_{IC}$ and G_{ICinit} were determined in this study.

EXPERIMENTAL

Materials

Unsized Hercules AS4 (trade name of Hercules, Inc.) graphite fibers having 3000 filaments per bundle were used in this study. These fibers ($\sim$ 7.2 μm in diameter) were coated with a thin layer of 3cmi-s via electropolymerization before they were fabricated into composites. A diglycidyl ether of bis-

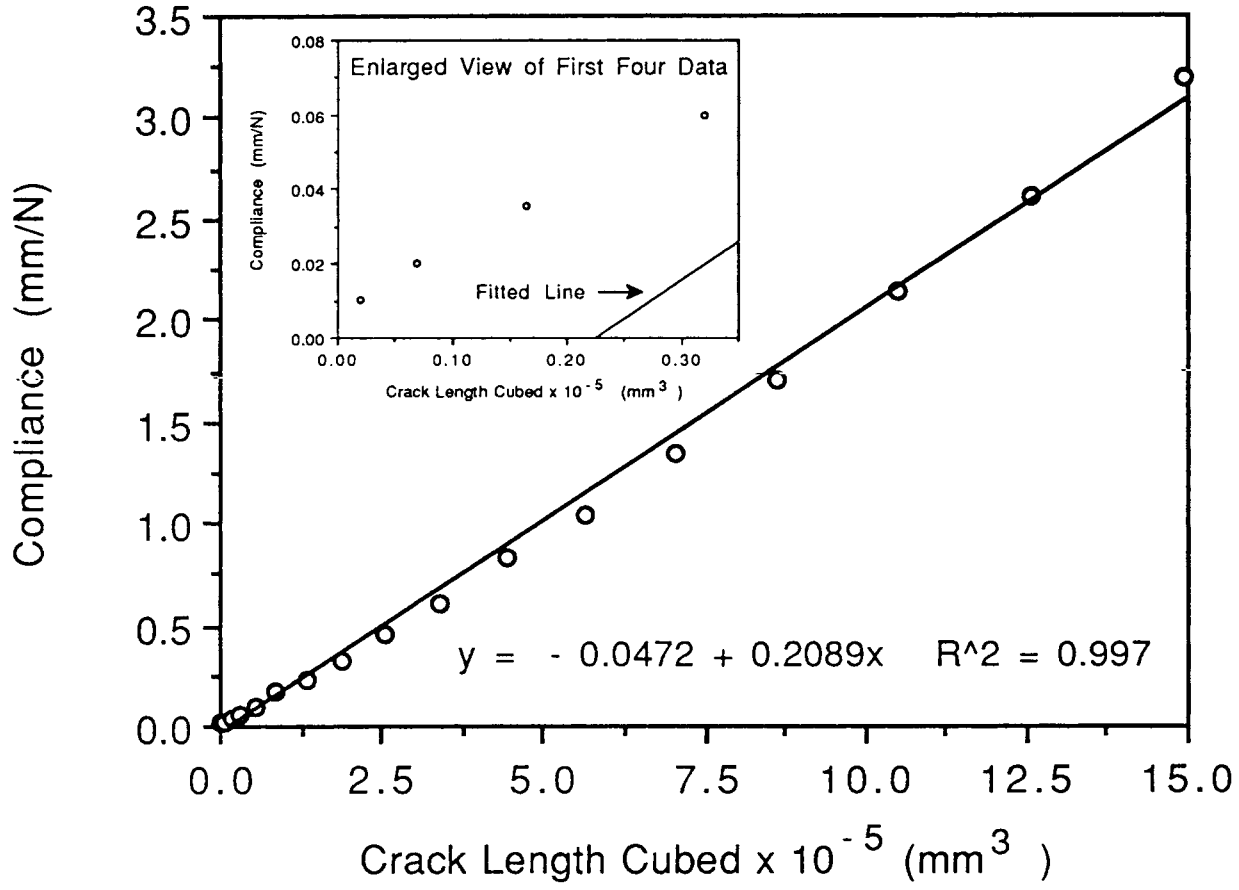

Figure 1 Straight line fitting of compliance vs. (crack length)^3 showing deviation at low crack length region.

phenol A [Epon (trade name of Shell Chemical Co.) 828] resin cured with a stoichiometric amount, 28 phr by weight, of 4,4'-methylenedianiline (MDA) was used as the matrix (tensile strength = 70 MPa and T_g = 168°C). The styrene monomers (Aldrich Chem. Co.) were vacuum distilled at about 50°C to remove the inhibitors. Only the middle portion of the distillate was collected and used. The 3-carboxyphenylmaleimide monomer (Mitsui Toatsu Chem., Inc.) was used as received.

Electrocopolymerization

Electrocopolymerization of 3cmi-s was conducted following the procedures previously described.[62] First, a solution was prepared consisting of approximately 40 : 60 volume ratio of dimethylacetamide–water co-solvent, 0.0125 mol/liter of H_2SO_4 in this co-solvent, and 0.0625 mol/liter each of the 3cmi and the styrene in the co-solvent. The solution was purged with N_2 for 5–10 min to remove any dissolved O_2. It was then transferred into the three-compartment electrocopolymerization cell. The solution was used in both the counterelectrode (anode) compartments as well as the working-electrode (cathode) compartment. About 20 g of fibers, carefully wound five layers thick onto a 152 × 203 mm (6 × 8 in.) rectangular aluminum frame, was then placed in the middle of the working-electrode compartment. The solution was circulated externally by pumping the solution out of the cell at one end and returning it at another end. The pump was circulating at about 400 mL/min. A constant-current density of 8.0 mA/g of fiber was then applied to the system to start the electrocopolymerization: 5 min to 1.5 h was used to obtain different coating thickness. An EG&G Princeton Applied Research Model 363 Potentiostat/Galvanostat was used to supply a constant current to the cell. After electrocopolymerization, the frame was removed from the bath, rinsed in a distilled water bath twice, and then dried in a vacuum oven at 250°C for 1 h to remove all residual dimethylacetamide. The frame was weighed again and any additional weight was taken to be the weight of the copolymer coating. The 3cmi-s copolymer obtained in this way has been found to be an alternating copolymer.[62,63]

Sample Preparation and Testing

Unidirectional Composite

Composites consisting of Hercules AS4 graphite fibers and Epon 828/MDA epoxy matrix were fabricated using a solvent impregnation technique.[1] Five layers of the fiber bundles were first wound onto a 152 × 203 mm (6 × 8 in.) frame, which usually yielded about 20 g of fibers on the frame. Epoxy resin matrix solution was then prepared by adding 10 g of acetone solvent to 18 g of epoxy resin–curing agent mixture. The acetone addition was to dissolve the MDA curing agent and to reduce the viscosity of the solution. The solution was then transferred via a disposable pipet onto the fibers. Acetone solvent was removed by placing the resin-coated fibers in a vacuum oven at room temperature for 30 min and at 80°C for 45 min. Essentially all acetone was removed this way, as indicated by the fact that the final weight loss is equal to the weight of acetone initially added.

After the vacuum oven treatment, the sample was cut into the shape of the mold (62 × 152 mm or 2.5 × 6 in.). For the coated fibers, the fibers were first removed from the frame and cut into the mold size before the resin solution was applied. Solvent removal was done in this case by hanging the coated plies on a ring stand with paper clips and placing the ring stand in the vacuum oven. Four parallel plies of the prepregs were then laid in the mold. If the composite fabricated was to be tested for G_{IC}, a thin 25.4-mm (1-in.) Teflon-coated cloth was inserted between the second and third plies to act as a crack initiator. The entire assembly was cured in the hot press at 80°C for 30 min under contact pressure. After that, additional pressure was applied and the curing continued at 80°C for 2 h. The temperature was then raised to 150°C and the curing continued at 150°C for 2 h. The hot press was then turned off, and the composite was allowed to cool overnight to room temperature. The composite was then postcured at 180°C for 2 h in an oven, and cooled slowly to room temperature. Pressure was always applied before the resin solidified in order to properly consolidate the composite plies. Pressure was used to control the resin flow and the fiber volume fraction.

G_{IC} Test Samples

The fabricated composites were cut into 25.4 × 152 mm (1 × 6 in.) G_{IC} test samples using a surface grinder (Brown & Sharp, Model 618 Micromaster), and a 0.81 mm (0.032 in.) diameter cutting wheel. Clean aluminum hinges were then adhered to the roughened composite surfaces using an Epon 828/Versamid 140 adhesive system in a 50 : 50 weight ratio. The adhesive was cured in an oven for 2 h both at 80 and 150°C, respectively. Silicone-grease release agent was applied to the unglued parts of the hinges so that the hinges could move freely. One

side of the sample was then painted with a typewriter correction fluid to aid in the crack growth observation. A strip of calibrated paper was also taped on the sample for easy crack length measurement.

Sample Testing

The DCB mode I test was conducted using an Instron Universal Tester at a crosshead speed of 0.1 cm/min. The crack length was observed with a 10X magnifying glass. A crack length increment of 6.35 mm (0.25 in.) was used. Two specimens were tested for each composite investigated, and average values are reported.

The impact resistance (IMPR) test was conducted on a Testing Machine Impact Tester (Model 52004) according to ASTM D256-87. Test specimens having a dimension of 63.5 mm long and 12.7 mm wide (2.5 × 0.5 in.) were cut from the fabricated composite using a surface grinder. The specimens were notched in the middle section with a 45° V-shape grinding wheel. The test was conducted by impacting the specimen with a 5-lb pendulum hammer at an impacting speed of 3.35 m/s (11 ft/s). The specimen's failure mode was also recorded. Five to eight specimens were tested for each composite investigated.

The short-beam interlaminar shear strength (ILSS) was determined on an Instron Model F/CML tester according to ASTM D2344-84. The width of the specimens was kept at 6.35 mm (0.25 in.). The length-to-thickness ratio was kept constant at 6 : 1, and the span-to-thickness ratio was 4 : 1. The crosshead speed was set at 0.1 cm/min. Nine to 16 specimens were tested for each composite investigated.

The fiber volume fraction, V_f, and the void content were determined using an acid digestion technique (ASTM D3171, Procedure A). A displacement technique as described in ASTM D792 was used to determine the composite's density. At least five samples, weighing about 0.5 g each, were used for each composite tested.

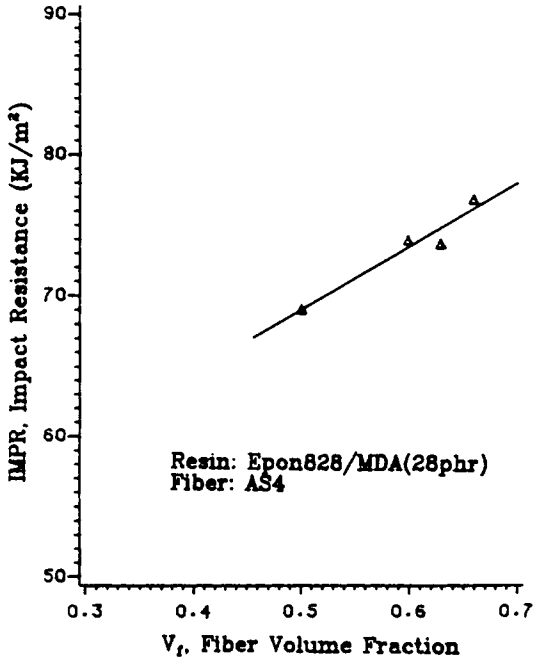

Figure 2 Impact resistance as a function of V_f for control composites; Ref. (1).

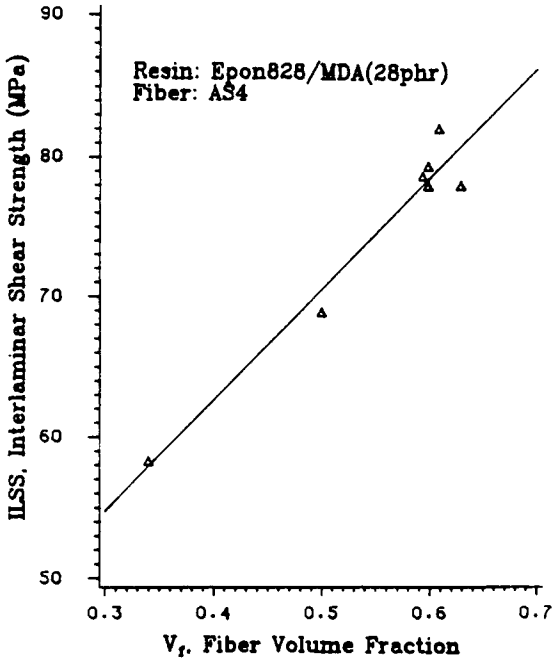

Figure 3 Interlaminar shear strength as a function of V_f for control composites; Ref. (1).

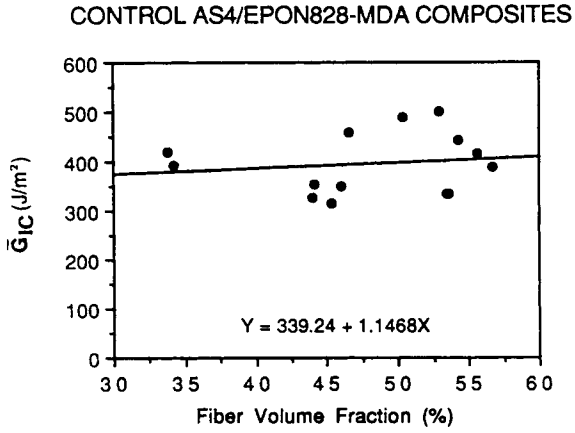

Figure 4 Average mode I critical strain energy release rate as a function of V_f for control composites.

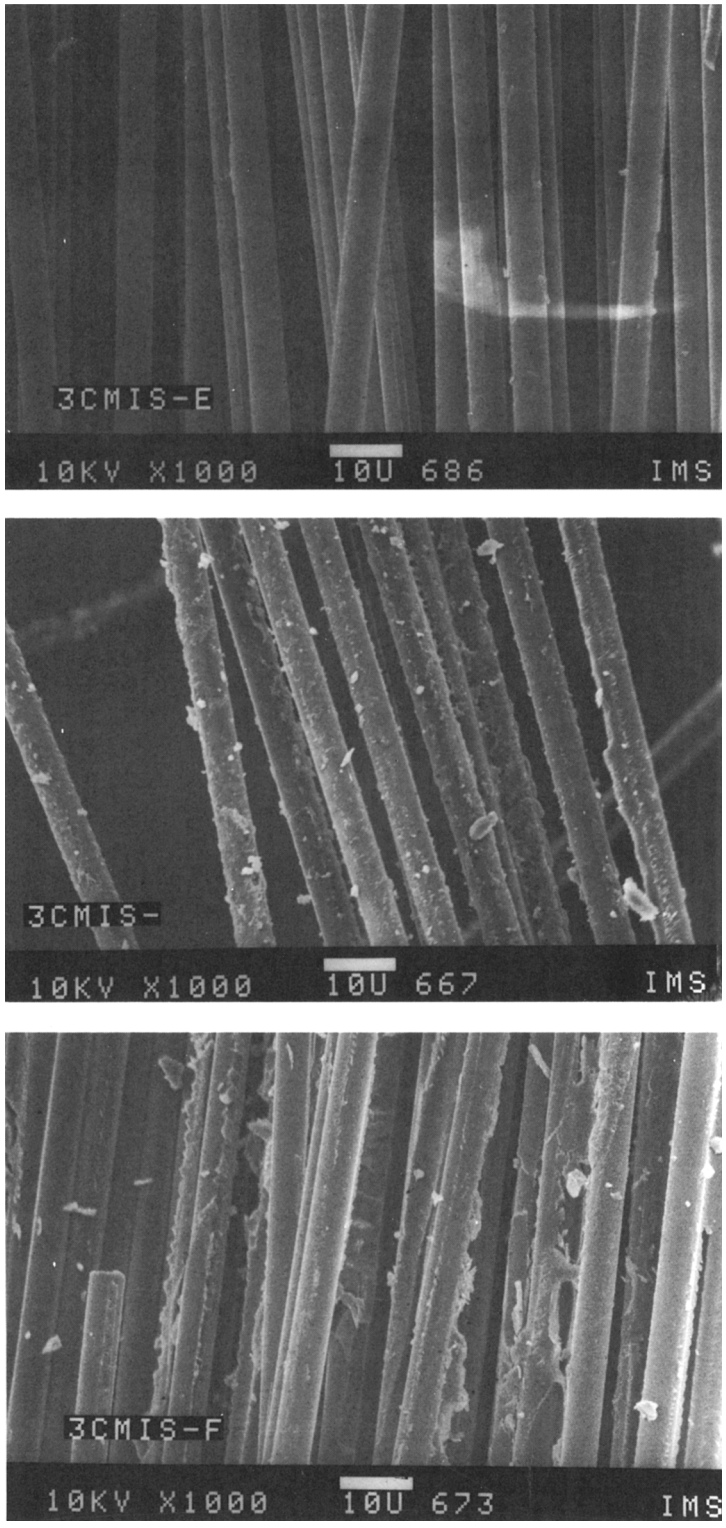

Figure 5 SEM micrographs of 3cmi-s coated fibers. (a) 3% interphase weight gain, (b) 10% interphase weight gain, (c) 27% interphase weight gain.

RESULTS AND DISCUSSION

V_f Normalization

The notched Izod impact resistance (IMPR) and the apparent interlaminar shear strength (ILSS) of the control AS4/Epon 828-MDA composites depend strongly on the fiber volume fraction (V_f). IMPR and ILSS increase linearly with increasing V_f.[1,2] On the other hand, the average critical strain energy release rate ($\bar{G}_{IC}$) is much less dependent on V_f. The effects of V_f on the IMPR, ILSS, and $\bar{G}_{IC}$ for the control uncoated composites are shown in Figures 2, 3, and 4, respectively. Figures 2 and 3 were reproduced from Chang's data.[1] Using the least-square technique, the following linear equations were found from Figures 2, 3, and 4, respectively:

$$\text{IMPR} = 46.53 + 0.45V_f \quad (2)$$

$$\text{ILSS} = 31.03 + 0.788V_f \quad (3)$$

$$\bar{G}_{IC} = 339 + 1.15V_f \quad (4)$$

IMPR, ILSS, $\bar{G}_{IC}$, and V_f have the units of kJ/m^2, MPa, J/m^2, and %, respectively. These three equations were used to normalize for the V_f effect so that the properties of the composites with and without the interphase could be compared at the same V_f. The normalization was done by taking the ratio of the property of the composite with the interphase (interphase composite) over the property of the control composite, at the same V_f. A normalized property of 1 means that there is no difference between the two composites. If the value is > 1, then there is some improvement, and if the value is < 1, there is some property reduction. The fiber volume fractions of 3cmi-s modified composites are in a similar range as the V_f range where Eqs. (2)-(4) were derived; therefore, minimal or no extrapolation was needed.

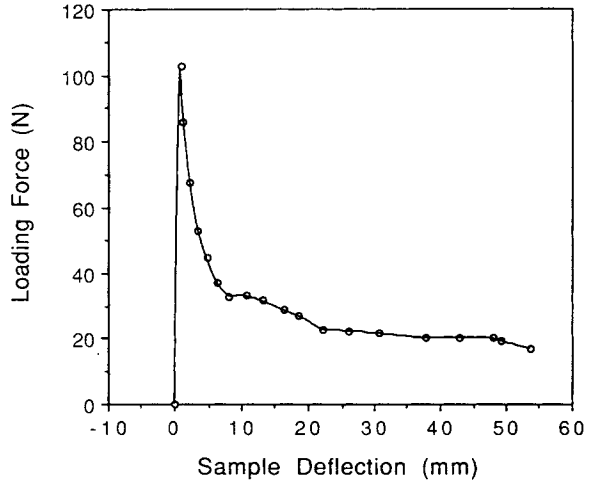

Figure 6 A typical G_{IC} load–deflection curve for control composites.

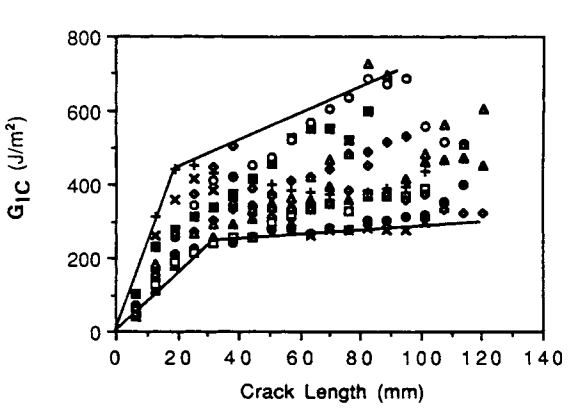

Figure 7 G_{IC} vs. crack length for various control composite specimens.

SEM of the 3cmi-s Interphase

The morphology of the 3cmi-s interphase is shown in Figures 5(a), 5(b), and 5(c) for 3, 10, and 27% interphase weight gain, respectively. The micrographs suggest that initially the 3cmi-s fibers were coated individually and had a smooth surface [Fig. 5(a)]. As the interphase thickness was increased to about 10% weight gain, the coated fibers began to stick to one another, most likely due to the narrow spacing between them. Grainy structures were observed on these 10% coated fiber surface. Fiber sticking became quite severe at 27% weight gain. At this thickness the coating behaves more like a matrix than an interphase. A polymer film appeared to be formed on the outer surface of the prepreg.

G_{IC} and Failure Modes

A typical load–deflection curve obtained from the DCB mode I test is shown in Figure 6. Initially, when the crack just started to propagate, the load decreased sharply with increasing deflection or increasing crack length. The crack propagation of 6.35 mm ($\frac{1}{4}$ in.) at this point took less than 30 s. As the deflection increased and the crack propagated further, the load continued to decrease, but at a slower rate. At crack lengths beyond 89 mm (3.5 in.), the load typically leveled off, and it took more than 3 min for the crack to propagate 6.35 mm. The crack

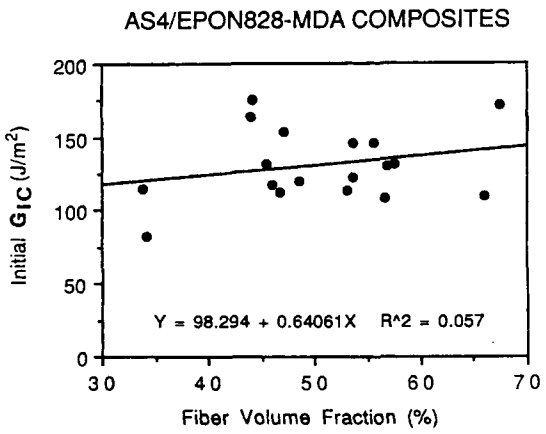

Figure 8 Initial G_{IC} as a function of V_f for control composites.

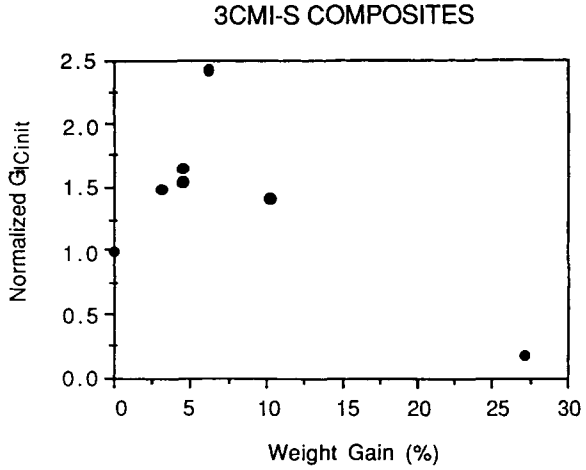

Figure 10 V_f-normalized initial G_{IC} vs. 3cmi-s weight gain.

propagation rate obviously decreased with increasing crack length.

A plot of G_{IC} versus crack length is given in Figure 7 for various control composites. The data were determined using a compliance method. The G_{IC} generally increased with increasing crack length (R-curve effect). The R-curve effect was observed for all specimens at crack lengths between 0 to about 30 mm. Beyond this crack length, the behavior varied from sample to sample. The G_{IC} of some samples leveled off to some constant value, but others continued to rise with increasing crack length. Some of the composites apparently have more fiber bridging than the others, since the R-curve effect is attributed to the fiber bridging across the delamination.

It has been suggested that the G_{IC} at the initial crack length is free of fiber bridging (because the fibers from one side of the beam were restricted from penetrating into the other side by the crack initiator cloth), and may provide additional understanding of the laminate toughness.[125] The initial G_{IC} for the control composites as a function of V_f is given in Figure 8. Similar to the $\bar{G}_{IC}$ behavior shown in Figure 4, the initial G_{IC} apparently is not a strong function of V_f. The numerical average G_{ICinit} was about 125 J/m^2, which was about one-third of the $\bar{G}_{IC}$ value. This 125 J/m^2 was very close to the neat epoxy resin G_{IC} value of 95 J/m^2, as reported in the literature.[107,122] The similarity of G_{ICinit} and neat resin G_{IC} was also found by other authors on similar systems.[107,128-130] These findings are not surprising since the region just behind the crack initiator cloth may consist of only the epoxy resin.

The load–deflection curves of the 3cmi-s coated

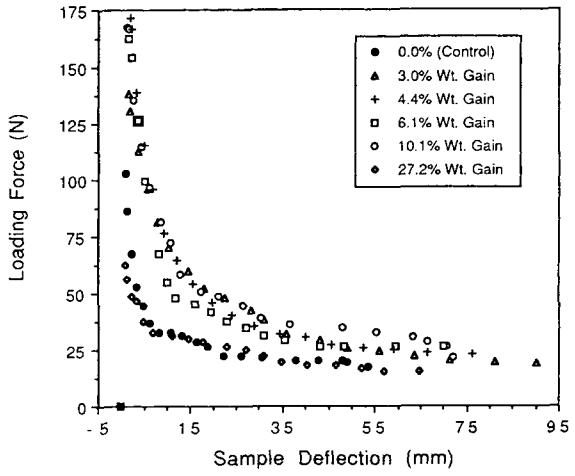

Figure 9 G_{IC} load–deflection curves of 3cmi-s composites.

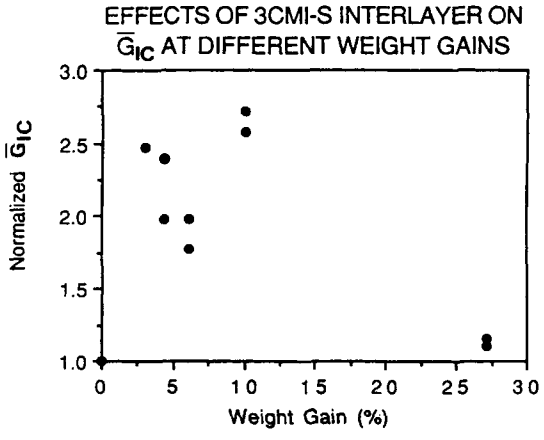

Figure 11 V_f-normalized average G_{IC} vs. 3cmi-s weight gain.

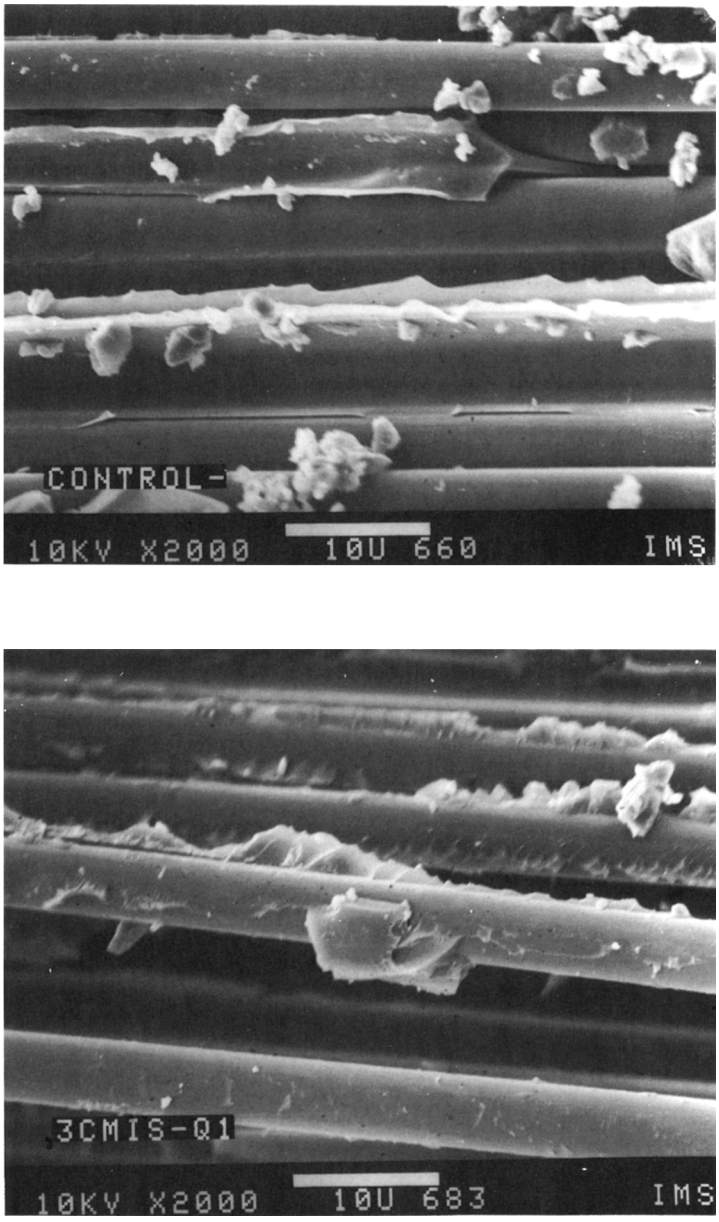

Figure 12 SEM micrographs of the G_{IC} failure surfaces. (a) control composite, (b) 6% interphase weight gain, (c) 10% interphase weight gain, (d) 27% interphase weight gain.

composites at different weight gain is shown in Figure 9. The control composite curve was also included for comparison purposes. The control composite showed a sharp load drop once the crack was initiated. In contrast, the load drop for the coated composites was more gradual. This suggests that the coated composites were more damage tolerant, i.e., the coated composites could withstand higher load after cracking. They also carried higher load at high sample deflection.

The V_f-normalized initial G_{IC} versus 3cmi-s weight gain is shown in Figure 10. G_{ICinit} increased with interphase thickness up to about 0.16 μm or about 6% weight gain. At this optimum thickness, about 150% improvement was found. This means that the 3cmi-s interphase had successfully toughened the composites and made the composites less sensitive to initiation delamination. After 6% weight gain, the G_{ICinit} decreased with increasing weight gain. The very low G_{ICinit} at 27% was most likely due to the severe fiber sticking as shown in Figure 5(c).

A plot of the V_f-normalized $\bar{G}_{IC}$ versus 3cmi-s weight gain is shown in Figure 11. All the normalized $\bar{G}_{IC}$ values are > 1. $\bar{G}_{IC}$ first increased with increasing

(c i)

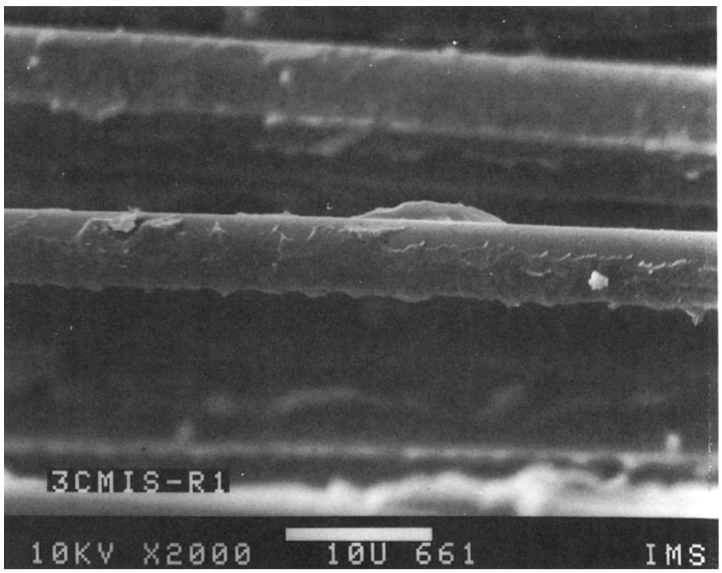

(c ii)

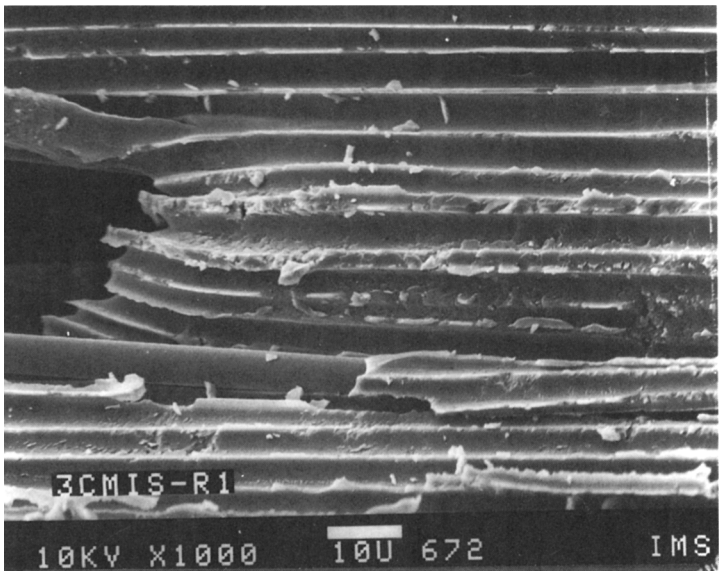

Figure 12 *(continued from the previous page)*

weight gain up to about 10%. It then decreased with further weight gain increase. This behavior was consistent with the results observed for the $\bar{G}_{IC}$ in the acrylic systems.[56] The 10% optimum weight gain was, however, different from the 6% found in the G_{ICinit} results. This higher 10% thickness may be due to the higher tolerance to fiber sticking when the crack was propagating rather than initiating. The higher tolerance, in turn, may be due to the presence of fiber bridging. At the optimum thickness, $\bar{G}_{IC}$ of the 3cmi-s composites was improved by about 160%.

The failure surface of composites (located 12.7 mm away from the initiator cloth) was analyzed by a scanning electron microscope (SEM), and the results for 0, 6, 10, and 27% 3cmi-s weight gain are given in Figures 12(a), 12(b), 12(c), and 12(d), respectively. The small spherical particles in the micrographs are debris from the sample cutting. As shown in Figure 12(a), the control composites have clean and orderly fracture surface, typical of brittle materials. Bare fiber surfaces with characteristic striations were found, indicating that the failure was at the fiber–matrix interface. The brittle matrix

(d i)

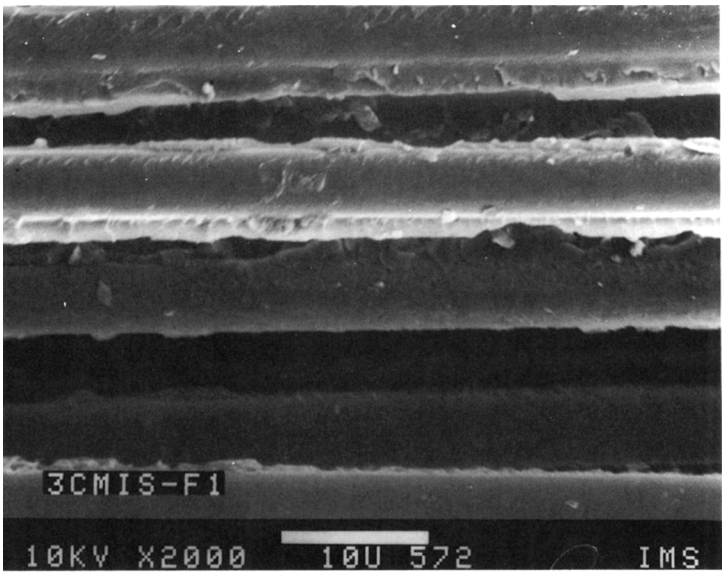

(d ii)

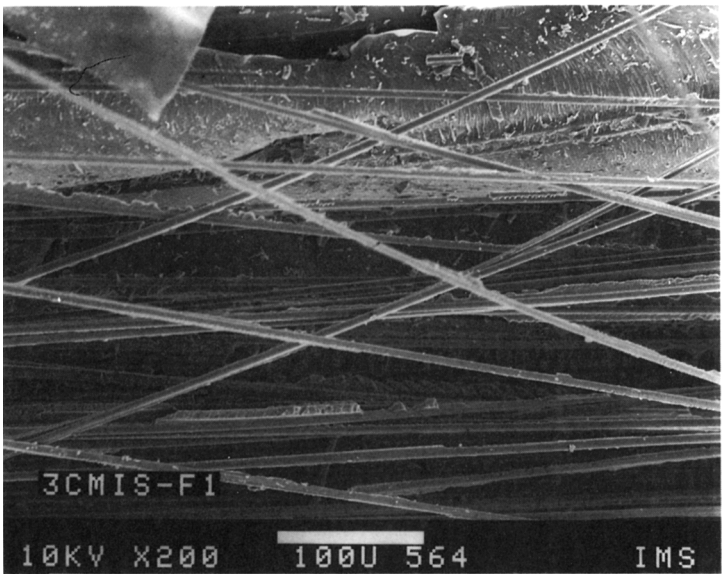

Figure 12 *(continued from the previous page)*

fracture in the micrographs is consistent with the low fracture energy found. With a 6% weight gain, the fracture surface changed dramatically [Fig. 12(b)]. The surface was rough and irregular. Some of the fibers have polymer adhering to them, while others have rather smooth surfaces with striations (characteristic of the uncoated AS4 fibers). Hackles, which were formed by shear components in the stress field, were observed throughout. The appearance of hackles correlates with the observed higher $\bar{G}_{IC}$. At 10% weight gain, rough and disorganized surfaces were found [Fig. 12(c)]. In addition to the interphase, matrix, and interfacial failures, matrix–interphase plastic deformation was also observed [Figure 12(c)(ii)]. This deformation appears to be in the tensile mode and is probably caused by the tensile stretching from fiber bridging. The high $\bar{G}_{IC}$ found at this interphase thickness is due to the high energy required to create the rough surfaces. Fractographs of 27% 3cmi-s composites are shown in Figure 12(d). Two types of failure surfaces are observed. The first is the rough surface found in Figure 12(d)(i). Compared to the clean failure in the control composite, more energy is probably required to generate this failure. The second is a filmlike failure surface found in Figure 12(d)(ii). This failure sur-

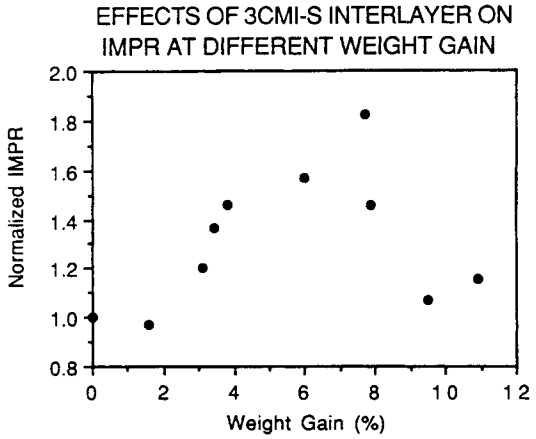

Figure 13 V_f-normalized impact resistance vs. 3cmi-s weight gain.

face is probably caused by the following. At 27% weight gain, a 3cmi-s film was formed at the prepreg's surface. In fabricating the composite, this film caused the epoxy to form an epoxy film at the interlaminar region. When the sample was tested, some cracks propagated at the interface between these two films, creating the observed filmlike feature.

Izod Impact Resistance

The normalized impact resistance versus the 3cmi-s weight gain is shown in Figure 13. Similar to the $\bar{G}_{IC}$ results, IMPR first increased with increasing weight gain up to about 6%. At the optimum thickness, about 60% improvement was found. This is twice as high as the improvement found in the acrylic interphases.[2] IMPR dropped with more weight gain after 6%. The IMPR improvement is probably because the interphase could act as an energy absorber, a crack arrester, and a stress delocalizer (increased the size of the deformation zone), thus resisting higher impact energy. The increase in the IMPR with increasing interphase thickness is probably due to the increase in the energy absorbing capacity and the increase in the deformation zone size ahead of the crack tip.

The macroscopic impact failure modes for the control and the 3cmi-s composites are given in Table I. As indicated, 8 out of 14 of the control composites broke completely into two pieces. On the other hand, at low interphase thickness, only 1 out of 6 of the 3cmi-s composites failed completely (the other 5 out of 6 failed partially with the upper and lower halves of the sample remained attached to one another). Between 3.4 and 7.9% weight gain, none of the samples failed by fracturing into two pieces. At 10.9% weight gain, 4 out of 6 of the samples again failed by fracturing into two pieces. There is apparently a positive correlation between the macroscopic failure modes and the observed IMPR property.

On the compression side of the sample away from the notch, two types of failure modes were observed; i.e., the 45° shear failure and the composite buckling failure, as shown in Figure 14. Only 45° shear failure was observed for the control composites. On the other hand, both types of failure were found for the interphase composites. In compression tests, buckling usually resulted in a bushy damage and a lower compression strength than clean 45° shear failure.[131] For toughness, however, more energy may be absorbed by buckling than by catastrophic shear failure, because buckling has the ability to withstand more strain, and more fibers can be debonded. The failure mode change may be attributed to the interphase being able to absorb more energy and increase the deformation zone size.

SEM micrographs of the failure surface for the control composites and the interphase composites have been taken. The interphase composite seems

Table I Percent of Impact Test Samples Having Macrosopically Complete Breakage

Sample Name	Weight Gain (%)	Number of Samples Tested	Number of Samples with Complete Failure	Sample with Complete Failure (%)
Bulk epoxy	—	8	8	100
Control	0.0	14	8	57
3cmis-I	1.6	6	1	17
3cmis-K	3.1	6	1	17
3cmis-C	3.4	6	0	0
3cmis-L	3.8	5	0	0
3cmis-T	7.9	6	0	0
3cmis-P	10.9	6	4	67

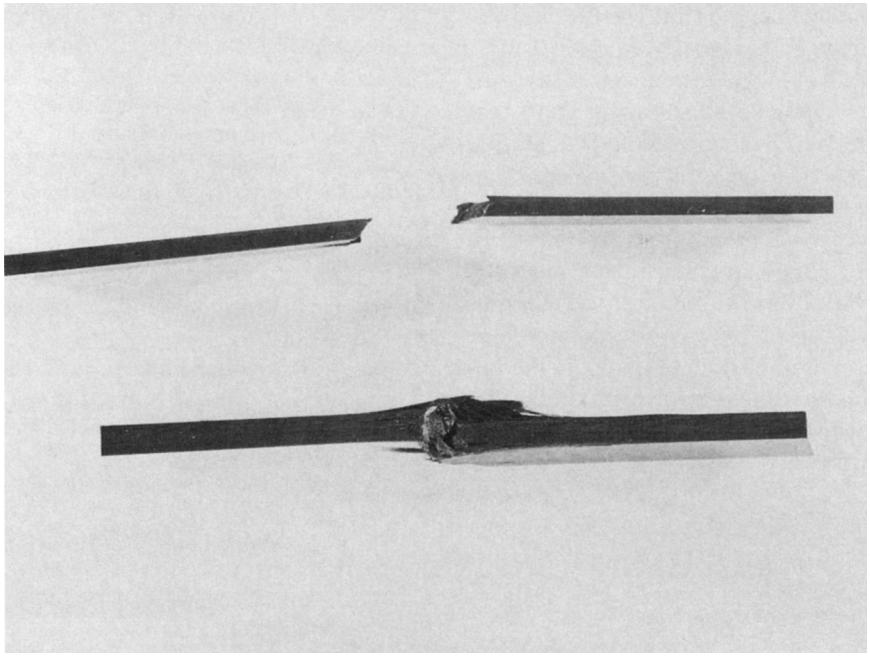

Figure 14 Specimens showing 45° shear failure and buckling failure.

to have more rough surface than the control. However, the failure surface of the two samples varied from location to location, i.e., clean surface as well as rough surface could be found in both samples. For this reason, no definitive conclusion can be made.

Short-Beam Interlaminar Shear Strength

The apparent interlaminar shear strength, ILSS, remains unchanged with the presence of the 3cmi-s up to 6%, as shown in Figure 15. After this thickness, ILSS decreases to below the control composite value. This is not unexpected because of the fiber sticking problem discussed earlier. In addition, the control AS4 fibers had been surface treated by the manufacturer to improve the fiber–epoxy adhesion. Thus the control composites already have good shear strength, and a large improvement in ILSS was not expected. The retention of ILSS up to 6% weight

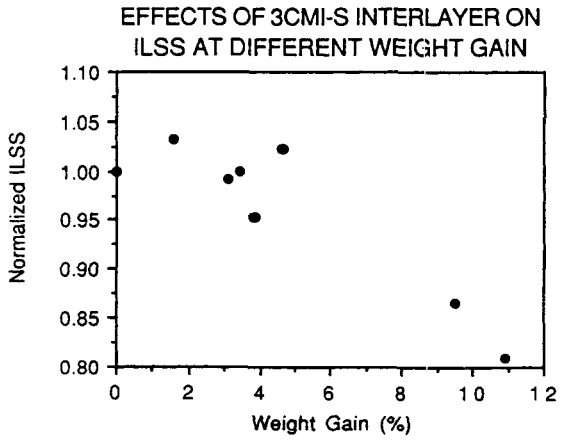

Figure 15 V_f-normalized interlaminar shear strength vs. 3cmi-s weight gain.

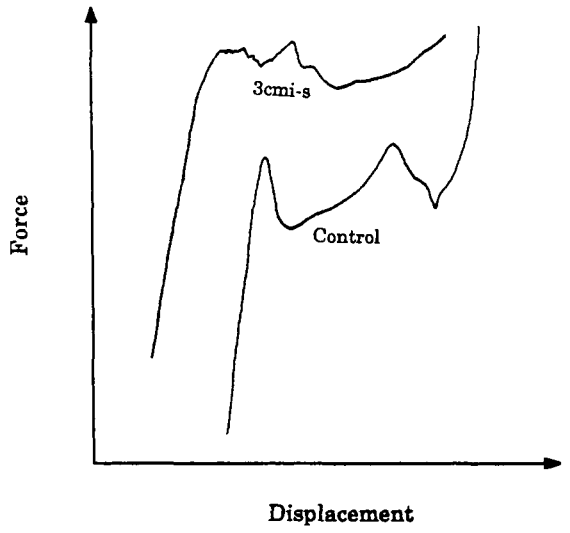

Figure 16 Comparison of short-beam shear force–displacement curves for control and 3cmi-s composites.

gain is acceptable, considering that the G_{IC} and the IMPR were improved substantially.

The force versus displacement curves of the control and the 3cmi-s composites from the ILSS test are shown in Figure 16. The 3cmi-s curve was shifted arbitrarily on the vertical scale for purpose of comparison. For the control composites, the force dropped sharply as soon as the sample failed. In contrast, the 3cmi-s composites retained almost the same force as the maximum value after the samples failed. This force retainment was also observed in the G_{IC} test as discussed earlier (Fig. 9). This behavior supports the toughness improvement results and indicates that the 3cmi-s composites have better damage tolerance.

CONCLUSIONS

Inclusion of the electrocopolymerized 3cmi-s interphase greatly toughened the AS4/Epon 828-MDA composites. The optimum interphase thickness is 0.16 μm (6% weight gain). At this optimum thickness, the DCB mode I critical strain energy release rate is improved by about 100%, the notched Izod impact resistance is improved by about 60%, and the apparent interlaminar shear strength is maintained at a similar value as the control composites. Fiber sticking, which restricted the even distribution of epoxy matrix, is probably the main reason for the property drops beyond the optimum thickness. The 3cmi-s modified composites failed in a more ductile mode than the control composites (more damage tolerance).

REFERENCES

1. J. Chang, Ph.D. Thesis, Univ. of Connecticut, Storrs (1986).
2. H. W. Rhee, Ph.D. Thesis, Univ. of Connecticut, Storrs (1987).
3. R. V. Subramanian and J. J. Jakubowski, *Polym. Eng. & Sci.*, **18**(7), 590–600 (1978).
4. R. V. Subramanian, V. Sundaram, and A. K. Patel, Proc. 33rd SPI RP/C Conf., Sec. 20-F (1978).
5. R. V. Subramanian and A. S. Crasto, *Polym. Compos.*, **7**(4), 201–218 (1986).
6. B. D. Agarwal and L. J. Broutman, *Analysis and Performance of Fiber Composites*, Wiley, New York, 1980.
7. A. G. Atkins, *J. Mater. Sci.*, **10**, 819 (1975).
8. R. S. Drake, *SAMPE Q.*, **6**, 11 (1980).
9. C. K. Riew, E. H. Rowe, and A. R. Siebert, *Adv. Chem. Ser.*, **154**, 326 (1976).
10. R. Y. Ting and R. J. Moulton, Proc. 12th Nat'l SAMPE Tech. Conf., October 7–9, p. 265 (1980).
11. J. Harper-Tervet, Proc. 27th Nat'l SAMPE Tech. Symp., May 4–6, p. 292 (1982).
12. S. L. Kirshenbaum and J. P. Bell, *J. Appl. Polym. Sci.*, **30**, 1875 (1985).
13. M. Ochi and J. P. Bell, *J. Appl. Polym. Sci.*, **29**, 1381 (1984).
14. Z. Nir, W. J. Gilwee, D. A. Kourtides, and J. A. Parker, *SAMPE Q.*, **14**, 34 (1983).
15. J. M. Scott and D. C. Phillips, *J. Mater. Sci.*, **10**, 551 (1975).
16. A. R. Seibert and R. S. Drake, Proc. 27th Nat'l SAMPE Tech. Symp., May 4–6, p. 739 (1982).
17. H. Wells and N. L. Hancox, Proc. 32nd Tech. Conf. SPI, Sec. 9-C (1977).
18. J. V. Larsen, Proc. 26th SPI RP/C Conf., Sec. 10-D (1971).
19. P. K. Mallick and L. J. Broutman, *J. Test. Eval.*, **5**, 190 (1977).
20. J. Summerscales and D. Short, *Composites*, **9**(3), 157 (1978).
21. P. W. R. Beaumont, P. G. Reiwald, and C. Zweben, in *Foreign Object Impact Behavior of Composites*, ASTM STP 568, 1974, p. 134.
22. D. Short and J. Summerscales, *Composites*, **11**(1), 33 (1980).
23. "Panel Discussion on: Thermoplastics Vs. Thermosets in Advanced Composites," *Polym. Compos.*, **8**(6), 437 (1987).
24. D. M. Carlin, Proc. 47th SPE Ann. Tech. Conf., Vol. XXXV, May 1–4, p. 1447 (1989).
25. U. Gaur, G. Desio, and B. Miller, Proc. 47th SPE Ann. Tech. Conf., Vol. XXXV, May 1–4, p. 1513 (1989).
26. A. Lustiger, Proc. 47th SPE Ann. Tech. Conf., Vol. XXXV, May 1–4, p. 1493 (1989).
27. J. Manson, S. Copeland, J. Seferis, and T. Schneider, Proc. 46th SPE Ann. Tech. Conf., Vol. XXXIV, April 18–21, p. 1598 (1988).
28. K. Quinn and G. O'Brien, Proc. 46th SPE Ann. Tech. Conf., Vol. XXXIV, April 18–21, p. 1617 (1988).
29. J. C. Seferis, *Polym. Compos.*, **7**, 158 (1986).
30. R. Pater and C. Morgan, Proc. 46th SPE Ann. Tech. Conf., Vol. XXXIV, April 18–21, p. 1639 (1988).
31. R. Pater, Proc. 47th SPE Ann. Tech. Conf., Vol. XXXV, May 1–4, p. 1434 (1989).
32. A. O. Hanky and T. L. St. Clair, *SAMPE J.*, **21**(4), 40 (1985).
33. A. H. Egli, L. L. King, and T. L. St. Clair, Proc. 18th Nat'l SAMPE Tech. Conf., Vol. 18, p. 440 (1986).
34. T. L. St. Clair, ACS Interdisciplinary Symp. on Recent Advances in Polyimides and Other High Temp. Polym., Reno, NV, July 13–16 (1987).
35. H. Zeng and K. Mai, *Macromol. Chem.*, **187**, 1787 (1986).
36. Y. Yamamoto, S. Satoh, and S. Etoh, *SAMPE J.*, **21**(4), 6 (1985).

37. P. A. Steiner, J. M. Browne, M. T. Blair, and J. M. McKillen, *SAMPE J.*, **23**(2), 8 (1987).
38. T. Pascal, R. Mercier, and B. Sillion, Proc. 3rd Inter. Conf. on Polyimides, Ellenville, NY, November 2–4 (1988).
39. S. Das, B. DeBona, and D. C. Prevorsek, Proc. SPE Regional Tech. Conf., Los Angeles, CA, November 15–17 (1988).
40. M. S. Sefton, P. T. McGrail, J. A. Peacok, S. P. Wilkinson, R. A. Crick, M. Davies, and G. Almen, Proc. 19th Nat'l SAMPE Tech. Conf., Vol. 19, p. 700 (1987).
41. R. S. Raghava, *J. Polym. Sci., Part B, Polym. Phys.*, **26,** 65 (1988).
42. R. D. Vannucci and K. J. Bowles, Proc. 17th Nat'l SAMPE Tech. Conf., Vol. 17, p. 352 (1985).
43. R. H. Pater, Proc. SPE Regional Tech. Conf., Los Angeles, CA, November 15–17, p. 273 (1988).
44. P. Delvigs, *Polym. Compos.*, **7**(2), 101 (1986).
45. R. H. Pater, *SAMPE J.*, **26**(5), 19 (1990).
46. J. P. Bell, J. Chang, H. W. Rhee, and R. Joseph, *Polym. Compos.*, **8**(1), 46 (1987).
47. J. Chang, J. P. Bell, and S. Shkolnik, *J. Appl. Polym. Sci.*, **34,** 2105 (1987).
48. G. Dagli and N. H. Sung, *Proc. ACS, Polym. Materials: Sci. Eng.*, **56,** 410 (1987).
49. A. S. Crasto, S. H. Own, and R. V. Subramanian, in *Composite Interfaces,* H. Ishida and J. L. Koenig, Ed., North-Holland, New York, 1986.
50. A. Benatar and T. G. Gutowski, *Polym. Compos.*, **7,** 84 (1986).
51. L. D. Tryson and J. L. Kardos, Proc. 36th SPI RP/C Conf., Sec. 2-E (1981).
52. R. E. Lavengood, M. J. Michno, and J. D. Fairing, Report AD-776-592, Monsanto Research Corp., March (1974).
53. E. P. Plueddemann, Ed., *Interfaces in Polymer Matrix Composites* (Vol. 6 of *Composite Materials,* L. J. Broutman and R. H. Krock, Eds.), Academic Press, New York, 1974.
54. J. L. Kardos, *ACS, Div. Polym. Chem. Polym. Prep.*, **24,** 185 (1983).
55. L. J. Broutman and B. D. Agarwal, *Polym. Eng. Sci.*, **14,** 581 (1974).
56. S. Wimolkiatisak, Ph.D. Thesis, University of Connecticut, Storrs (1990).
57. A. S. Wimolkiatisak and J. P. Bell, *Polym. Compos.*, **10**(3), 162 (1989).
58. A. S. Crasto, S. H. Own, and R. V. Subramanian, *Polym. Compos.*, **9**(1), 78 (1988).
59. W. W. Wright, *Compos. Polym.*, **3**(4), 231 (1990).
60. W. W. Wright, *Compos. Polym.*, **3**(5), 360 (1990).
61. P. S. Theocaris, *The Mesophase Concept in Composites,* Springer-Verlag, Berlin, 1987.
62. J. Iroh, J. P. Bell, and D. A. Scola, *J. Appl. Polym. Sci.*, **41,** 735 (1990); Proc. SPE's RETEC, November 14–17, Los Angeles, CA (1988).
63. J. P. Bell, J. Iroh, W. Kim, and D. Scola, Proc. 47th SPE Ann. Tech. Conf., Vol. XXXV, May 1–4, p. 565 (1989).
64. J. R. MacCallum and D. H. MacKerron, *Eur. Polym. J.*, **18,** 717 (1982).
65. J. R. MacCallum and D. H. MacKerron, *Brit. Polym. J.*, **14,** March, 14 (1982).
66. W. H. Kim, M.S. Thesis, Univ. of Connecticut, Storrs (1988).
67. W. R. Grace and Co., Brit. Pat. 1,156,309, June 25 (1969).
68. R. Dijkstra and J. De Jonge, Sci. Technol. Surf. Coat., NATO Adv. Study Inst., p. 85, (1972) (Publ. 1974).
69. C. Iwakura, M. Tsunaga, and H. Tamura, *Electrochim. Acta,* **17,** 1391 (1972).
70. F. Bruno, M. C. Pham, and J. E. Dubois, *Electrochim. Acta,* **22,** 451 (1977).
71. V. N. Epimakhov, Y. M. Mishenov, and B. I. Yudkin, *Plast. Massy,* **9,** 74 (1975).
72. D. C. Phillips, S. Spewock, and W. M. Alvino, *J. Polym. Sci. Chem. Ed.*, **14,** 1137 (1976).
73. D. C. Phillips and W. M. Alvino, *J. Polym. Sci. Chem. Ed.*, **14,** 1157 (1976).
74. N. Yamazaki, *Adv. Polym. Sci.*, **6,** 377 (1967).
75. K. Hamann, *Makromol. Chem.*, **99,** 103 (1966).
76. A. F. Diaz, K. K. Kanazawa, and G. P. Gardini, *J. Chem. Soc. Chem. Commun.*, **14,** 635 (1979).
77. E. M. Genies, G. Bidan, and A. F. Diaz, *J. Electroanal. Chem.*, **149,** 101 (1983).
78. J. Bargon, S. Mohmand, and R. J. Waltman, *Mol. Cryst. Liq. Cryst.*, **93,** 279 (1983).
79. J. Bargon, S. Mohmand, and R. J. Waltman, *IBM J. Res. Dev.*, **24,** 330 (1983).
80. J. L. Bredas, R. Sibley, and D. S. Boudreaux, *J. Am. Chem. Soc.*, **105,** 6555 (1983).
81. K. E. Creasy and B. R. Shaw, *Anal. Chem.*, **61**(13), 1460 (1989).
82. T. F. Guarr and F. C. Anson, *J. Phys. Chem.*, **91**(15), 4037 (1987).
83. J. M. Calvert, R. H. Schmehl, B. P. Sullivan, J. S. Facci, T. J. Meyer, and R. W. Murray, *Inorg. Chem.*, **22**(15), 2151 (1983).
84. C. P. Horwitz and R. W. Murray, *Mol. Cryst. Liq. Cryst.*, **160,** 389 (1988).
85. B. L. Funt, Electrochemical Initiation, in *Encyclo. of Polym. Sci. and Eng.*, Vol. 5, 2nd Ed., Wiley, New York, 1987, p. 587.
86. R. V. Subramanian, *Adv. Polym. Sci.*, **33,** 33 (1979).
87. B. L. Funt and J. Tanner, in *Technique of Electroorg. Synthesis Part 2,* N. L. Weiberg, Ed., Vol. 5, Wiley, New York, 1975.
88. B. L. Funt, *Macromol. Rev.*, **13,** 37 (1967).
89. J. Zak and T. Kawana, *J. Electroanal. Chem., Interfacial Electrochem,* **150** (1–2) 645 (1983).
90. R. W. Murray, *Acc. Chem. Res.*, **13,** 135 (1980).
91. R. W. Murray, in *Electroanal. Chem.*, A. J. Bard, Ed., Vol. 13, Marcel Dekker, New York, 1984.
92. K. D. Snell and A. G. Keenan, *J. Chem. Soc. Chem. Soc. Rev.*, **8**(2), 259 (1979).

93. W. J. Albery and A. R. Hillman, *Chem. Soc. Ann. Rep. Prog. Chem., Sec.-C,* **78,** 377 (1982).
94. P. Denisevich, H. D. Abruna, C. R. Leidner, T. J. Meyer, and R. W. Murray, *Inorg. Chem.,* **21**(6), 2153 (1982).
95. G. Mengoli, *Adv. Polym. Sci.,* **33,** 1 (1979).
96. J. W. Breitenbach and C. Srna, *Pure Appl. Chem.,* **4,** 245 (1962).
97. C. L. Wilson, in *Encyclo. of Electrochem.,* Reinhold, New York, 1964.
98. H. Z. Friedlander, in *Encyclo. Polym. Sci. & Technol.,* Vol. 5, Wiley, New York, 1971, p. 629.
99. S. M. Wenz and J. Mijovic, *SAMPE J.,* March/April, 31 (1986).
100. D. Purslow, *Composites,* **15**(3), 207 (1984).
101. D. Purslow and R. Childs, *Composites,* **17**(2), 127 (1986).
102. J. M. Tang, W. I. Lee, and G. S. Springer, *J. Compos. Mater.,* **21,** May, 421 (1987).
103. G. S. Springer, *J. Compos. Mater.,* **16,** September, 400 (1982).
104. T. G. Gutowski, Z. Cai, S. Bauer, D. Boucher, J. Kingery, and S. Wineman, *J. Compos. Mater.,* **21,** July, 650 (1987).
105. A. J. Russell and K. N. Street, in *Progress in Sci. and Eng. of Compos.,* T. Hayashi, K. Kawata, and S. Umekawa, Eds., ICCMIV, Japan Soc. for Compos. Mater., Tokyo, 1982, p. 279.
106. A. J. Russell and K. N. Street, in *Delamination and Debonding of Materials,* W. S. Johnson, Ed., ASTM STP 876, ASTM, Philadelphia, 1985, p. 349.
107. A. J. Russell and K. N. Street, in *Toughened Composites,* N. J. Johnston, Ed., ASTM STP 937, ASTM, Philadelphia, 1987, p. 275.
108. R. Joseph, J. P. Bell, and H. W. Rhee, *Polym. Eng. Sci.,* **28**(9), 605 (1988).
109. G. J. Becht and J. W. Gillespie, Jr., *Polym. Compos.,* **10**(5), 293 (1989).
110. D. J. Wilkins, NAV-GD-0037, Naval Air System Command (1981).
111. W. S. Johnson and P. D. Mangalgiri, in *Toughened Composites,* N. J. Johnston, Ed., ASTM STP 937, ASTM, Philadelphia, 1987, p. 295.
112. J. G. Williams, *J. Compos. Mater.,* **21,** April, 330 (1987).
113. S. Mall, G. E. Law, and M. Katouzian, *J. Compos. Mater.,* **21,** June, 569 (1987).
114. A. J. Russell, *Polym. Compos.,* **8**(5), 342 (1987).
115. S. M. Lee, *J. Compos. Mater.,* **20,** March, 185 (1986).
116. S. Lee, P. C. Gaudert, R. C. Dainty, and R. F. Scott, *Polym. Compos.,* **10**(5), October, 305 (1989).
117. R. A. Crick, D. C. Leach, P. J. Meakin, and D. R. Moore, *J. Mater. Sci.,* **22,** 2094 (1987).
118. W. D. Bascom, D. J. Boll, B. Fuller, and P. J. Phillips, *J. Mater. Sci.,* **20,** 3184 (1985).
119. A. J. Smiley and R. B. Pipes, *J. Compos. Mater.,* **21,** July, 670 (1987).
120. S. L. Donaldson, *Composites,* **16**(2), 103 (1985).
121. J. A. Hinkley, N. J. Johnston, and T. K. O'Brien, NASA Tech. Memo. 100532, USAAVSCOM TM 88-B-002, February, (1988); J. A. Hinkley, *J. Reinf. Plast. Compos.,* **9,** 470 (1990).
122. D. L. Hunston, R. J. Moulton, N. J. Johnston, and W. D. Bascom, in *Toughened Composites,* N. J. Johnston, Ed., ASTM STP 937, ASTM, Philadelphia, 1987, p. 74.
123. J. M. Whitney, C. E. Browning, and W. Hoogsteden, *J. Reinf. Plast. Compos.,* **1,** October, 297 (1982).
124. D. J. Wilkins, J. R. Fisemann, R. A. Camin, W. S. Margolis, and R. A. Bension, in *Damage in Compos. Mater.,* ASTM STP 775, 1982, p. 168.
125. J. A. Hinkley, submitted for ACS Advances in Chem. Series Book *Composites,* based on Symp. Sponsored by Macromolecular Secretariat at the ACS Nat'l Meeting, Anaheim, CA, Fall (1986).
126. J. A. Hinkley, private communication, 1988.
127. S. Wu, *Polymer Interface and Adhesion,* Marcel Dekker, New York, 1982, Chapter 14, p. 556.
128. J. M. Whitney, in *Interlaminar Response of Compos. Mater.,* N. J. Pagano, Ed., Vol. 5 of Compos. Mater. Series, Elsevier, Amsterdam, 1989.
129. H. Chai, *Eng. Fract. Mech.,* **24,** 413 (1987).
130. W. S. Johnson and P. D. Mangagiri, *Compos. Technol. Rev.,* Spring, 10 (1987).
131. D. Hull, *An Introduction to Composite Materials,* Cambridge Univ. Press, Cambridge, U.K., 1981, p. 154.

Received August 7, 1991
Accepted January 29, 1992